TECHNICAL REPORT
NATICK/TR-09/010

AD _____

A SHOCK TUBE FOR DOWNSELECTING MATERIAL CONCEPTS FOR BLAST PROTECTION PART I: DESCRIPTION OF THE SHOCK TUBE AND A COMPARISON OF FLUSH MOUNTED AND RECESS MOUNTED PRESSURE SENSORS

by
Ronald A. Segars
and
Marina G. Carboni

December 2008

Final Report
October 2002 – June 2008

U.S. Army Natick Soldier Research, Development and Engineering Center
Natick, Massachusetts 01760-5000

DISCLAIMERS

The findings contained in this report are not to be construed as an official Department of the Army position unless so designated by other authorized documents.

Citation of trade names in this report does not constitute an official endorsement or approval of the use of such items.

DESTRUCTION NOTICE

For Classified Documents:

Follow the procedures in DoD 5200.22-M, Industrial Security Manual, Section II-19 or DoD 5200.1-R, Information Security Program Regulation, Chapter IX.

For Unclassified/Limited Distribution Documents:

Destroy by any method that prevents disclosure of contents or reconstruction of the document.

REPORT DOCUMENTATION PAGE

Form Approved
OMB No. 0704-0188

PLEASE DO NOT RETURN YOUR FORM TO THE ABOVE ADDRESS.

1. REPORT DATE *(DD-MM-YYYY)*	2. REPORT TYPE	3. DATES COVERED *(From - To)*
11-12-2008	Final	October 2002 – June 2008

4. TITLE AND SUBTITLE

A SHOCK TUBE FOR DOWNSELECTING MATERIAL CONCEPTS FOR BLAST PROTECTION--PART I: DESCRIPTION OF THE SHOCK TUBE AND A COMPARISON OF FLUSH MOUNTED AND RECESS MOUNTED PRESSURE SENSORS

5a. CONTRACT NUMBER

5b. GRANT NUMBER

5c. PROGRAM ELEMENT NUMBER

6. AUTHOR(S)

Ronald A. Segars and Marina G. Carboni

5d. PROJECT NUMBER

IV.SP.2004.01

5e. TASK NUMBER

5f. WORK UNIT NUMBER

7. PERFORMING ORGANIZATION NAME(S) AND ADDRESS(ES)

Natick Soldier Research Development and Engineering Center
ATTN: AMSRD-NSR-WS-CM
Natick, MA 01760-5000

8. PERFORMING ORGANIZATION REPORT NUMBER

NATICK/TR-09/010

9. SPONSORING / MONITORING AGENCY NAME(S) AND ADDRESS(ES)

10. SPONSOR/MONITOR'S ACRONYM(S)

11. SPONSOR/MONITOR'S REPORT NUMBER(S)

12. DISTRIBUTION / AVAILABILITY STATEMENT

Approved for public release; distribution is unlimited.

13. SUPPLEMENTARY NOTES

14. ABSTRACT

This report documents Part I of a study on the interaction between shock waves and material systems as part of a U.S. Army initiative to better protect individual Soldiers against novel blast threats. The research was conducted using a shock tube fabricated at the U.S. Army Natick Soldier Research, Development and Engineering Center (NSRDEC). The shock tube was used because it is less expensive than explosive blasts, allows many tests to be obtained in a short time, offers much better repeatability, and can be operated in a laboratory setting. The primary goal of its use was to identify appropriate test procedures and evaluation criteria for the initial screening and down selection of material systems that have potential to provide blast protection, subsequently enabling evaluation of down selected systems in true blast environments. The work reported here was designed to answer some of the questions involved in measuring pressure behind flexible fabrics, such as the effect of sensor mounting (flush mounted versus recessed) and the effect of sample thickness or areal density on the pressure measurement. Several analyses were performed to correlate theoretical calculations with the observed measurements. The results indicate that the shock tube worked properly and that all sensors responded appropriately. The data from this study suggest that careful consideration must be given to appropriate mounting of materials with respect to pressure sensors for measurement. The degree of contact between sensor and material may have a significant effect on results.

15. SUBJECT TERMS

BLAST	PRESSURE	EXPLOSIVES	SHOCK WAVES	OVERPRESSURE
SENSORS	WEAPONS	SHOCK TUBE	BLAST WAVES	THREAT REDUCTION
FLEXIBLE	LETHALITY	PENETRATION	STRESS WAVES	WOUNDS AND INJURIES

16. SECURITY CLASSIFICATION OF:			17. LIMITATION OF ABSTRACT	18. NUMBER OF PAGES	19a. NAME OF RESPONSIBLE PERSON
a. REPORT	b. ABSTRACT	c. THIS PAGE			Marina Carboni
U	U	U	SAR	28	19b. TELEPHONE NUMBER *(include area code)* (508) 233-5461

This page intentionally left blank.

Table of Contents

List of Figures

List of Tables

Preface

This work reported here was performed by the U.S. Army Natick Soldier Research Development and Engineering Center as part of an Army Technology Objective (ATO) *Individual Protection Against Novel Blast Threats*, under Project Number IV.SP.2004.1 during the period October 2002 to June 2008. The end goal of the ATO was to characterize the threat from novel explosives with current body armor and to develop a blast protective concept against primary blast lung injury. Understanding the variation in threat, if any, between conventional and novel explosives along with identifying the energy transfer mechanisms within the material and the body was important to the development of protective equipment. As part of the ATO, material evaluation using a shock tube was explored as a technique to understand the interaction of shock waves and subsequent stress wave propagation through material. Shock tubes have been used by many researchers to evaluate materials and protective concepts, yet controversy on the accuracy of the measurement techniques and tools used exists. The work reported here contributed to the end goal by exploring methods to evaluate material concepts using pressure sensors within a shock tube.

A SHOCK TUBE FOR DOWNSELECTING MATERIAL CONCEPTS FOR BLAST PROTECTION--PART I: DESCRIPTION OF THE SHOCK TUBE AND A COMPARISON OF FLUSH MOUNTED AND RECESS MOUNTED PRESSURE SENSORS

1 Introduction

Whenever new weapons are fielded, whether foreign or domestic, those in charge of protecting Soldiers must take up the challenge to reduce the threat these weapons create. Recent threats come from novel blast weapons specifically designed to generate overpressures high enough to cause severe internal injury and lethality. In general, explosive shock waves are particularly effective in rooms, near walls, and in trenches where reflections enhance the effective overpressure and duration (Phan and Stollery)[1].

Development of the optimum protection for a Soldier in blast environments requires knowledge of how blast waves interact with material and material systems. It also requires an understanding of how the shock wave, or stress wave, propagates through the materials, enters the body, and inflicts injury on the internal organs.

This report documents part of a larger study on the interaction between shock waves and material systems. This work was performed by the U.S.. Army Natick Soldier Research, Development and Engineering Center (NSRDEC) as part of an Army Technology Objective (ATO) *Individual Protection Against Novel Blast Threats.* A shock tube was used to conduct the research. There are many advantages to performing small scale laboratory testing with a shock tube instead of explosive blasts. It is less expensive, allows many tests to be obtained in a short time, offers much better repeatability, and can be operated in a laboratory setting. The primary goal of its use was to identify appropriate test procedures and evaluation criteria for the initial screening and down selection of material systems that have potential to provide blast protection. Down selected systems could then be evaluated in true blast environments.

Shock tubes have been used by several researchers to evaluate the effect of materials on the transmission of shock waves (Skews [2, 3], Gelfand [4], Gibson [5], Winfree [6]). Although much work had been performed, understanding pressure sensor measurements underneath flexible material systems and the relationship of these measures to risk of injury was uncertain. For instance, Skews showed that a small space between the fabric and the endplate gave rise to wave reflections and an increase in pressure far above what would have occurred had the material not been present. However, he did not study the case where the material was in contact with the sensor surface. To investigate the question of direct contact versus an air space, NSRDEC fabricated an endplate with two pressure sensors. One was mounted flush with the endplate surface, and the second was recessed 2 mm from the surface. The data described in this report were collected using this endplate. Subsequent reports will cover other gages and a variety of sample mounting techniques, which are discussed in Section 2.2. The ultimate goal

was to provide the optimum method for using a shock tube to measure the shock wave (overpressure) attenuation capability of material systems.

The work reported here was designed to answer some of the questions involved in measuring pressure behind flexible fabrics. Of particular interest was investigating the effect of sensor mounting, flush mounted versus recessed, and the effect of sample thickness or areal density on the pressure measurement. The materials and experimental methods used are described in Chapters 2 and 3, respectively. The results of the analyses are discussed in Chapter 4, and the conclusions drawn from those results are presented in Chapter 5.

2 Materials

2.1 The Shock Tube

A small shock tube was fabricated and set up in laboratory space at NSRDEC. The design of the shock tube was constrained by size, space, and location criteria. It needed to be small enough for safe laboratory operation, without producing excessive noise.

The shock tube (shown in Figure 1) was constructed from a stainless steel pipe 6.72 cm I.D. and 7.28 cm O.D. The driver section is 30.5 cm long with a 1.27 x 12.5 cm stainless steel flange at each end. The flanges have six equally spaced holes for 3/8 in x 1 3/4 in hardened bolts. Overall, the driver section was designed to withstand a pressure of 27.5 MPa (4000 psi), which was near the yield pressure of the stainless steel tube. A 1.27 x 2.5 cm stainless steel plate, with a 1/4 in NPT threaded hole in the center to bring in the high-pressure gas, covers the inlet end of the driver. The driven section was 183 cm long with flanges similar to those used on the driver section at both ends. In Figure 1 the three side-on pressure sensor taps were located on the right side of the driven section at 5.08 cm, 15.24 cm, and 25.4 cm from the flange. (i.e., Locations 2, 5, and 1, respectively, shown in Figure 2). The initial endplate used for the driven section (discussed further in Section 2.2) was a 1.27 x 12.5 cm stainless steel plate with two pressure sensor taps 3.18 cm center to center, symmetrically located with respect to the tube walls (i.e., Locations 3 and 4 shown in Figure 2). The pressure tap in Location 3 was flush with the surface of the end plate; the pressure tap in Location 4 is recessed 2 mm from the end plate surface.

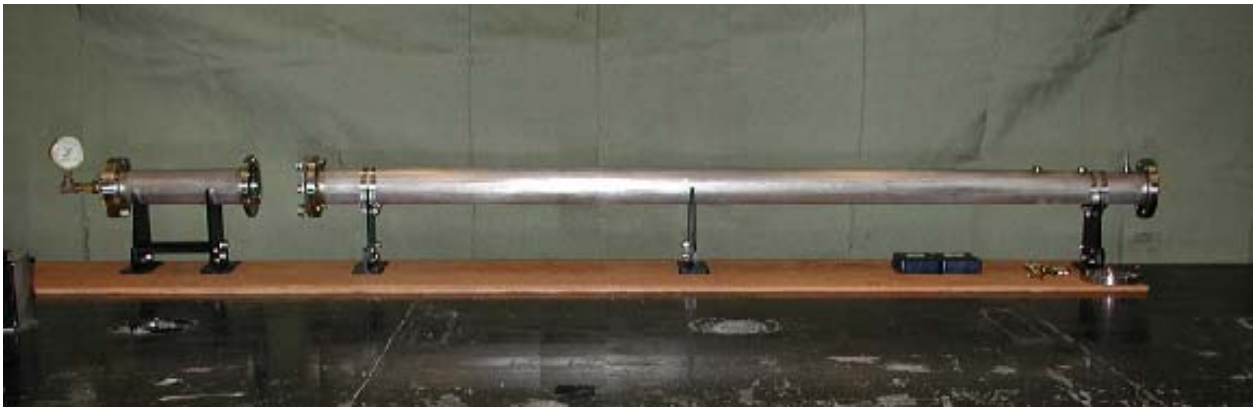

Figure 1: Photograph of the shock tube.

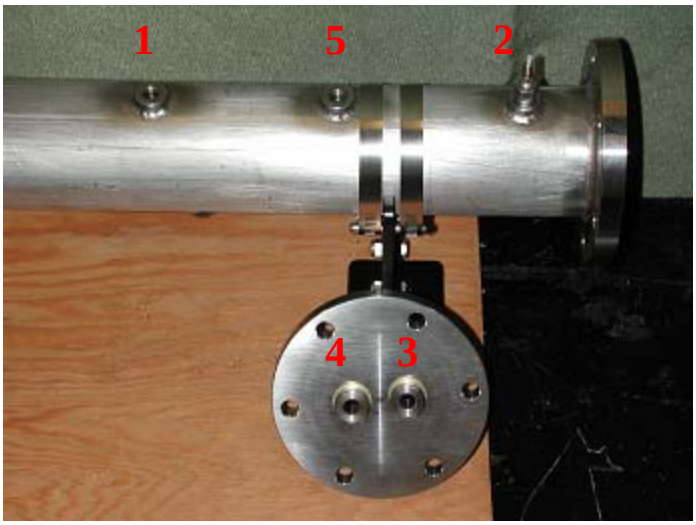

Figure 2: Endplate and pressure sensor mounts

The pressure to load the driver section and rupture the diaphragm was provided by a 20 gallon SPEEDAIRE (Dayton Electric Manufacturing Co.) industrial duty air compressor. This 1 HP compressor has a maximum working pressure of 690 kPa. A pressure gage was mounted in the inlet line of the driver section to monitor the driving pressure until the time the diaphragm burst. The shock tube has no built-in mechanism to rupture the diaphragm; thus, the driver pressure depends on the rupture strength of the diaphragm material. Pressure sensors (PCB model 102A06) were mounted in the three pressure taps on the walls of the driven section (Locations 1, 5, and 2 of Figure 2) to measure the side-on pressures ahead of the endplate. These pressure sensors are acceleration compensated, high frequency piezoelectric sensors with a maximum pressure rating of 3.45 MPa. The sensing plate is 5.54 mm in diameter. Two pressure sensors (PCB model 113A26) were mounted in the end-plate (Locations 3 and 4 of Figure 2) and measured the reflected pressure at the endplate surface. These pressure sensors have the same characteristics as those in the tube wall, but were mounted using o-rings with the o-rings and sensor press fit into the endplate. The signals from the pressure transducers were sent to a PCB model 482A22 signal conditioner and then on to a Win600 eight-channel data processing system. Measurements of time (in seconds) and voltage from the pressure transducers were recorded.

The Win600 software displayed the pressure traces, saved the recorded data, and provided the digitized values required for the theoretical analyses. A typical set of traces displayed on the Win600 screen is shown in Figure 3. Only four pressures were recorded; pressure at the middle sensor in the tube wall was not monitored. The top trace (P1) was from the sensor in the tube wall nearest the diaphragm; it was the one first seen by the shockwave. The second trace (P2) was from the sensor in the tube wall nearest the endplate. The third trace (P3) was the reflected pressure measured by the sensor flush mounted in the endplate. The fourth trace (P4) was the reflected pressure from the recessed sensor.

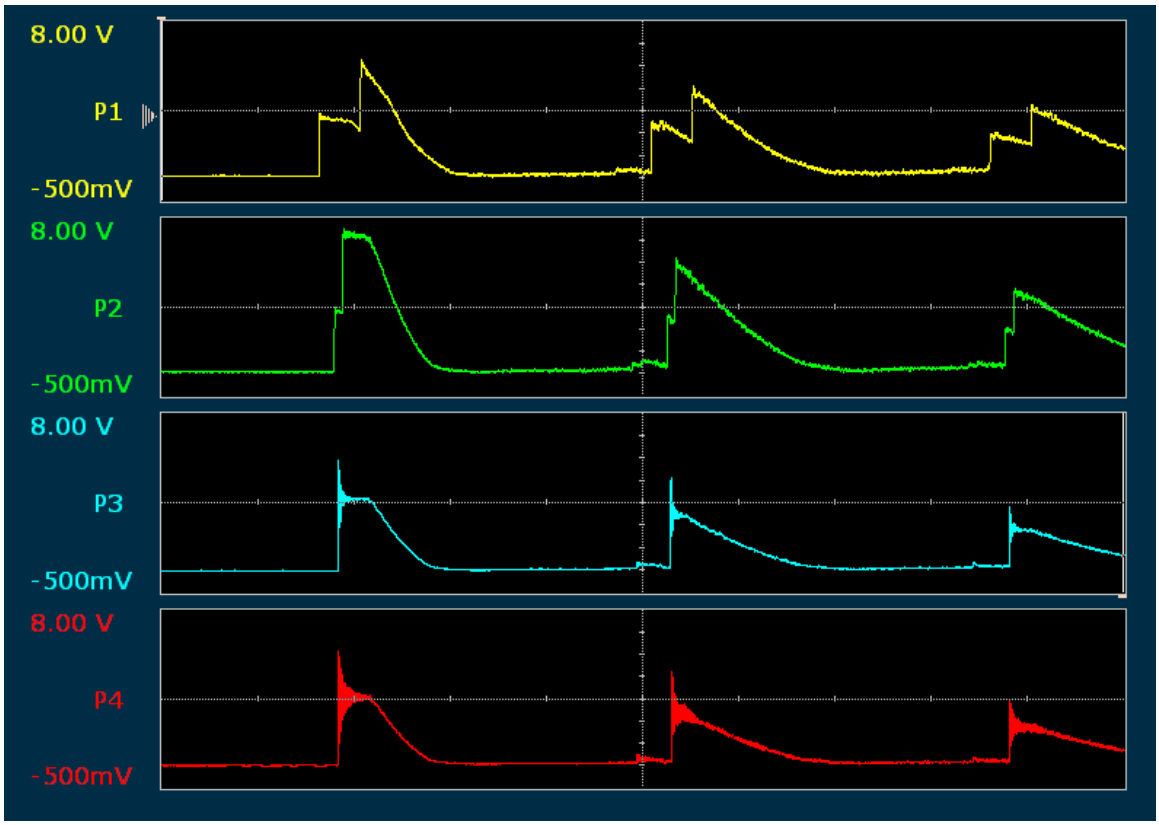

Figure 3: Typical traces displayed on the screen of the Win600; bare plate.

2.2 Endplates

Several different endplates were used with this shock tube as part of the effort to develop a relationship between shock tube and explosive testing for the evaluation of a material system's protective capability. Various problems and questions that surfaced throughout experimentation were investigated. All of the endplates and modifications that were used with the shock tube are given in Table 1. Only the work with the first endplate (Endplate I) is reported here. Subsequent reports will cover other gages and a variety of the sample mounting techniques listed in Table 1. Endplate I was designed to examine the differences in pressure measurements underneath flexible fabric systems due to contact with the sensing element. As described in Section 2.1 one sensor (P3) was flush mounted to achieve direct contact with the material, and the other (P4) was recessed 2 mm below the surface. From this setup the effect of contact on the pressure measurements should have been observable. A second function of this setup was to enable determination of whether the cavity acts as an air gap and, as theory predicts, reduces the magnitude and perhaps the frequency content of the transmitted pressure.

Table 1: Endplates and modifications that were used with the shock tube.

Endplate	Description
I	Two pressure sensors equally spaced across the horizontal shock tube I.D.: • One mounted flush with the surface of the endplate • The other recessed 2 mm below the surface of the endplate
II	Endplate I with the recessed sensor replaced with a flush mounted force gage
III	Endplate II with modifications to force gage mounts: • Mod 1: A stainless steel ring to fill the 2 mm gap between the force gage plate and the walls of the endplate • Mod 2: Addition of small screws to hold the ring in place • Mod 3: Enhancements to ensure the ring did not make contact with the sensing plate • Mod 4: Modification of the back surface of the ring so that it did not touch and preload the force gage housing.
IV	Endplate III with Mod 4, used for materials testing with a force gage
V	Endplate I with the recessed sensor only 0.11 mm below the endplate surface
VI	A single pressure sensor that is flush mounted at the center of the shock tube exit

2.3 Test Materials

Commercially available aluminum foil, Saran Wrap, and various plastic wraps were evaluated to determine an adequate burst diaphragm. The materials used to investigate the differences in sensor measurements were three different open cell packing foams, Kevlar® fabric, and aluminum foil. The materials were cut to fit the inner diameter of the shock tube (6.72 cm). A list of these materials along with some important material properties are given in Table 2. The determination of sound speed is described in Section 3.2.

Table 2: Properties of the materials evaluated.

Material	Density kg/m^3	Areal Density kg/m^2	Sound Speed m/s	Acoustic Impedance kg/m^2s
Blue Foam	96.0	0.610 (0.25 in)	210±60	20160
Green Foam	93.7	0.595 (0.25 in)	580±77	54346
Gray Foam	24.5	0.155 (0.25 in)	315	7718
Kevlar® Fabric	740.9	0.218 (1-layer)	41.9	31035
Aluminum Foil	1918	0.047 (1-layer)	5090	9762620

3 Methods

3.1 Shock Tube Performance and Measures

As outlined in Section 2.1, four pressure traces (P1, P2, P3, and P4) were recorded for each test. Incident side-on pressures P1 and P2 and the reflected pressures (Pr1 and Pr2) measured at side-on taps 1 and 2 were recorded from traces P1 and P2 in Figure 3. The reflected pressures from the endplate, P3 and P4, were also recorded.

Initially, a series of tests was performed to select a diaphragm material that would produce repeatable overpressures for material evaluation. Subsequent testing showed that using two layers of aluminum foil was the appropriate choice. As a diaphragm it produced an average overpressure of 37.01 ± 4.55 kPa with a total range over 44 shots of 24.57 to 43.59 kPa. Although this range was quite large a closer look at the pressures shows that 75% of the data are within the range 35.49 to 41.68 kPa. A calculation of the Mach number shows the two layers of aluminum foil provided a weak shock with an average Mach number of 1.146 and a Mach number range from 1.099 to 1.170. In general, the aluminum foil diaphragm produced consistent shock strengths and was used for the remaining experimentation.

Testing without materials was then performed with the selected diaphragm to generate a baseline performance and to correlate various shock tube parameters and sensor measurements. J.R. Wright, (p 32)[7] provides an equation for determining the strength of the shock wave, in terms of its pressure ratio, based on the pressure in the driving chamber at the time the diaphragm bursts. The pressure in the driving chamber as measured by the dial gage mounted in the inlet to the chamber was 124.1 ± 34.5 kPa. At this pressure, calculation from Wright's equation estimates the shock pressure ratio (absolute pressures) to be 1.474. Averaging over 44 shots the pressure ratio at the first tap, which was 1.576 m downstream from the diaphragm, was 1.365. Considering the distance from the diaphragm this was reasonable agreement. As a further check on the performance of the shock tube, the theoretical arrival time of the expansion wave at the first pressure tap was determined. These calculations followed the procedure outlined by LaPlante et.al. [8]. Although the full duration of the initial shock could not be seen at P1 due to the arrival of the wave reflected from the endplate, the expected arrival time of the expansion wave agreed well with the time at which decay of the initial shock began.

Lastly, the Rankine-Hugoniot equations relating the Mach number to the pressure change across a normal shock were also used to characterize shock tube performance. The shock velocity, derived from the Mach number calculated at P1, was used to predict the arrival time of the shock at P2 and at the endplate. The side-on pressures (P1 and P2) were also used to predict the reflected pressures (P3 and P4) at the endplate. This analysis is discussed in Chapter 4.

3.2 Sensor and Material Evaluation

Using the selected diaphragm, tests were performed with no materials against the endplate (bare) and with the materials described in Table 3. Several thicknesses (areal densities) of each material were subjected to a shock wave, and the resulting pressure measurements from Taps 1-4 were recorded. The material specimen was positioned into the open end of the shock tube, where contact with the endplate surface was made once the endplate was bolted on. The foam disks

were held in place by the friction against the tube walls while the aluminum foil and the Kevlar® were taped to the endplate. Only one sample from each material was used for evaluation, and the number of exposures for a material varied from one to seven.

In addition to analyzing the various pressure ratios across the samples, calculations based on the reflectance-transmittance conditions at an interface were performed to estimate expected pressures downstream of the various materials (Thompson, p 190) [9]. These equations are based on the knowledge that the pressures and particle velocities are constant across an interface. This simple calculation gives a good estimate of the pressure expected at the endplate.

The sound speeds for the three foams given in Table 2 were obtained from the difference in arrival time of the shock (pressure wave) at the front of the material and at P3. The shock velocity was calculated from the pressure ratio at P1 using 344 m/s as the speed of sound in air. From these calculations the travel time to the material front surface and through the material was obtained and hence the wave speed in the material determined. These values are much higher than the values obtained from the quasi-static modulus and density due in part to the viscoelastic nature of these materials and the high rate of impact from the shock tube. The wave speed for Kevlar® fabric was obtained by measuring the transverse elastic modulus through in-house compression measurements taken on a 28 layer disk of Kevlar fabric. The initial slope of the stress-strain compression curve gave an elastic modulus of 1.3 MPa. The density of the sample was 740.9 kg/m^3. The value for aluminum foil was derived from the bulk properties of aluminum. Subjecting these samples to a shock wave, monitoring the appropriate pressures, and applying the calculations described above provides a data base of information on the response of pressure sensors when they are covered by flexible material.

4 Results and Discussion

Voltage traces similar to those in Figure 3 were converted to pressure traces and are plotted in Figure 4. Only the first wave shown in the traces of Figure 3 were plotted. From data plots such as these it is easy to obtain the peak, average, and reflected pressures for each sensor. The arrival times of the incident shock and the reflected shock at each sensor were also easily obtained and provide good measures of transit times and shock velocity. Initial decay of the incoming shock is seen in the pressure trace for P1. Decay started before the reflected wave returned from the endplate. This start time coincided with the calculated time of arrival of the rarefaction wave. The traces for P3 and P4 show significant oscillations behind the shock front. The oscillations for the recessed sensor (P4) were larger and had a longer duration. These oscillations disappeared when the material was placed in front of the endplate; their cause is unknown.

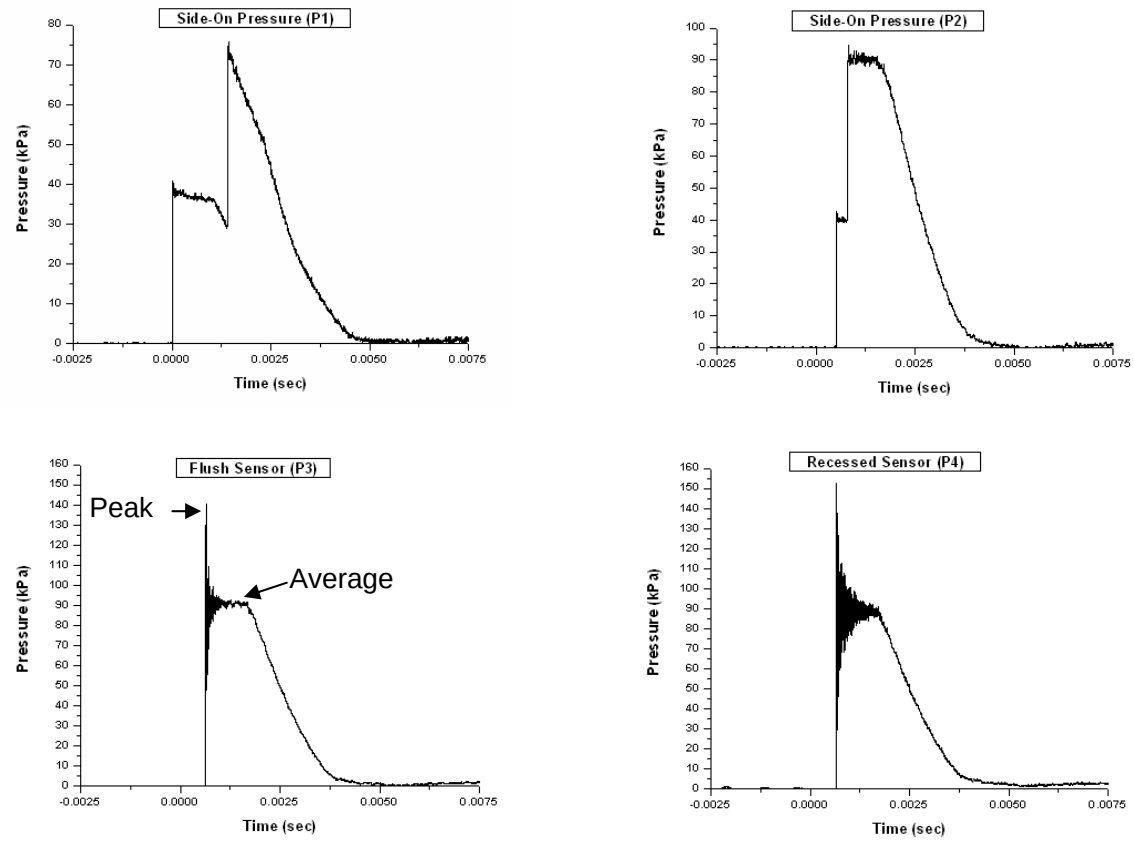

Figure 4: A typical set of data obtained from the four pressure taps (P1, P2, P3 and P4) with no materials in the shock tube (bare endplate).

Calculations of the expected pressure ratios (Pr2/P2) based on the acoustic approximation at interfaces, for all of the materials and conditions tested, are compared with their observed pressure ratios in Table 3. Included in Table 3 are the total number of tests run at each condition and the number of tests used in obtaining averages. The data from several of the tests could not be used because the peak pressure for P3 was clipped in those tests. The acoustic impedance of these materials (listed in Table 2) was high in comparison with the acoustic impedance of air. As a result, the reflected pressures were nearly the same for all conditions and were within the

accuracy of the measurements. All of the materials reflected similar to the bare endplate alone and to each other. Therefore, the pressure transmitted into the materials was essentially the same for all materials and thicknesses tested. The predicted values for the gray foam do not agree well with the observed data. This discrepancy cannot be ascribed to uncertainties in acoustical impedance, since this would require unreasonable impedance values. Some unexpected behavior such as compression of the foam undoubtedly occurred. The effect of compression on acoustic behavior is unknown. It should be noted that these data points are from only one shot per material thickness and therefore, are not representative of a population sample.

Table 3: Materials and thicknesses tested, number of replications, usable replications, and calculated and observed reflected pressure ratios (Pr2/P2).

Material	Total Replications	Replications Used	Pr2/P2 Calculated	Pr2/P2 Observed
Bare	7	7	2	2.182
Aluminum Foil	2	2	2	2.197
Blue Foam_.25in	3	2	1.962	1.997
Blue Foam_.5in	1	1	1.962	2.259
Blue Foam .75in	1	1	1.962	2.087
Blue Foam 1in	2	2	1.962	2.053
Green Foam_.25in	4	3	1.986	1.901
Green Foam_.5in	3	2	1.986	1.914
Green Foam_.75in	4	3	1.986	2.009
Green Foam_1.25in	1	1	1.986	1.978
Green Foam_1.5in	2	2	1.986	1.940
Gray Foam_.5in	1	1	1.902	1.551
Gray Foam_1in	1	1	1.902	1.590
Gray Foam _2in	1	1	1.902	1.209
Kevlar_1layer	2	0	1.998	2.079
Kevlar_5layers	3	2	1.998	1.964
Kevlar_10layers	1	1	1.998	2.004
Kevlar_15layers	3	3	1.998	2.081
Kevlar_5L_.25B Foam	2	1	1.998	1.958

Comparisons between the theoretical and observed estimates of the arrival time of the shock wave were used to verify the sensor response. The observed peak pressure range for P1 (24.57 kPa to 43.59 kPa) has a Mach number range of 1.099 to 1.170. The transit time from P1 (T1i) to the bare endplate (T3r) was estimated from the respective Mach numbers of each test and the speed of sound in air of 344 m/s (at atmospheric pressure and temperature of 70.4° F). The arrival time at the endplate was in excellent agreement with the estimated value. For example, a test where the shock pressure was 5.44 psi had a shock Mach number of 1.148. The shock velocity of 395 m/s (c=344 m/s) gave an arrival time at the endplate of 0.648 ms. The observed arrival time was 0.650 ms. Transit time was also calculated for tests with the various samples in front of the endplate. Wave speed in the material was obtained as described in Section 3.2. The

strength of the reflected waves was determined from the wave speeds, the density of the material, and the acoustic approximation. The wave speed relative to the flow and to the tube wall was determined from the strength of the reflected wave (Mach number). These speeds and the distance to be traveled provided the time of arrival (T1r) of the reflected wave at P1. Although theory (Beranek [10]) shows that sound speed is frequency dependent and will generally cause dispersion in the stress wave, reasonable agreement is seen between the calculated values and those observed. The results of the arrival time calculations are shown in Figure 5. The initial shock wave velocity was determined from P1, the velocity of the reflected shock was based on the acoustic approximation at the material surface, and calculated time was plotted versus the observed arrival time.

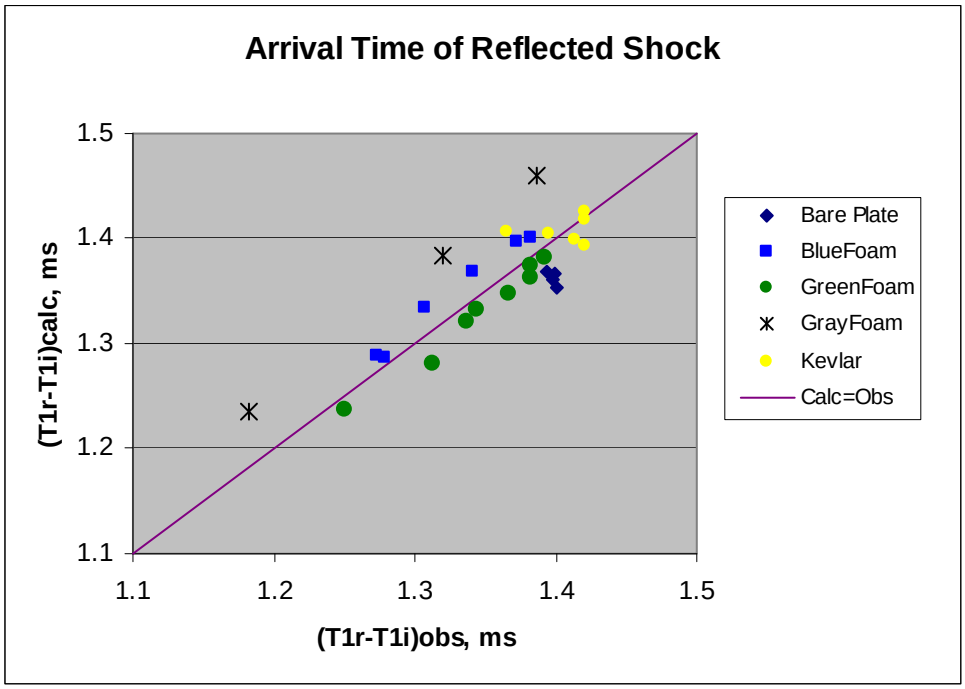

Figure 5: Arrival time at P1 of the shock wave reflected from the front surface of the material.

The initial study with the shock tube focused on the question of how to measure pressure behind a flexible fabric and to evaluate the importance of contact between the sensing surface and a flexible material. To investigate the effect of contact, the areal density of each test system was used as the independent variable so that all materials and thicknesses could be shown on the same plot. The three pressures downstream from P1 were normalized for shock strength by forming the ratio Pi/P1, i=2,3,4. Both peak pressures and an average pressure were used as test parameters. The average pressure was obtained from the region between the peak pressure and the point where the arrival of the expansion wave started the pressure decay.

It should be pointed out that the number of data points in a plot for a particular material may not be consistent from plot to plot and may not agree with the n in Table 3. In some cases P3 was clipped, and the peak pressure was not captured. The average pressure at P3 was still within the range of the settings and was recorded. Several times two data points were so close together that they appeared as a single point on the graph. The reflected pressure expected at the endplate when it was covered by a material with an acoustic impedance far below that of steel was

approximately four times the incoming pressure P1. This assumes close contact between the material and the steel plate (P3). If an air gap exists between the material and the steel plate (P4), the expected pressures would be very low.

The pressure ratios P3/P1 and P4/P1 tended toward their expected values as the areal density increased. Figures 6 and 7 show the behavior of the peak pressures as a function of the areal density for the flush mounted and recessed sensors, respectively. For three materials, the blue, the green foam and Kevlar®, the flush sensor had a slight decrease or nearly constant value at low areal densities followed by a significant increase in peak pressure as the areal density increased above some material dependent value. The gray foam was not tested at the higher areal densities, and therefore, it is not known whether it would have shown this increase. Figure 7 shows that the recessed sensor measured a monotonically decreasing pressure, or a sudden drop in pressure followed by a nearly constant value as the areal density increased. The aluminum foil in front of the sensors increased the peak pressure above the bare plate value. This may have been due to an increased effective area, particularly for the recessed sensor where the foil could compress the air in the cavity. However, the average pressure behind the aluminum foil agreed well with the bare plate result. When a thin layer (0.25 in.) of blue foam was placed between five layers of Kevlar® and the sensors, the flush sensor (P3) read a higher pressure than either the Kevlar® or foam produced alone. The recessed sensor (P4) read a pressure that was quite close to the blue foam alone at the same areal density. This pressure was lower than for Kevlar® at the same areal density. The difference in peak pressure response between the flush mounted and recessed sensors is not understood. For the flush mounted sensor there is only a single data point, and its high value may be due to scatter. The average pressures read by these sensors, for a given areal density, seems to depend on the contacting surface. The average pressures agreed more closely with the open cell blue foam than the closely woven Kevlar®, particularly for the recessed sensor (P4).

These trends are generally followed by the average pressures shown in Figures 8 and 9. However, the average pressure for Kevlar® is not as affected by the change in areal density as the peak pressure. Also, the average pressure for the foam-backed Kevlar® shows that both P3 and P4 measurements are very close to the blue foam alone at the same areal density.

In Figures 10 and 11 the difference in pressure recorded by the flush mounted and recessed sensors, respectively, normalized by P1 are plotted against the areal density. It appears that as the areal density increases the difference in peak and average pressure (P3-P4) between the two sensors increases. Again, for Kevlar® the difference in average pressure was affected less by areal density than by the peak pressure.

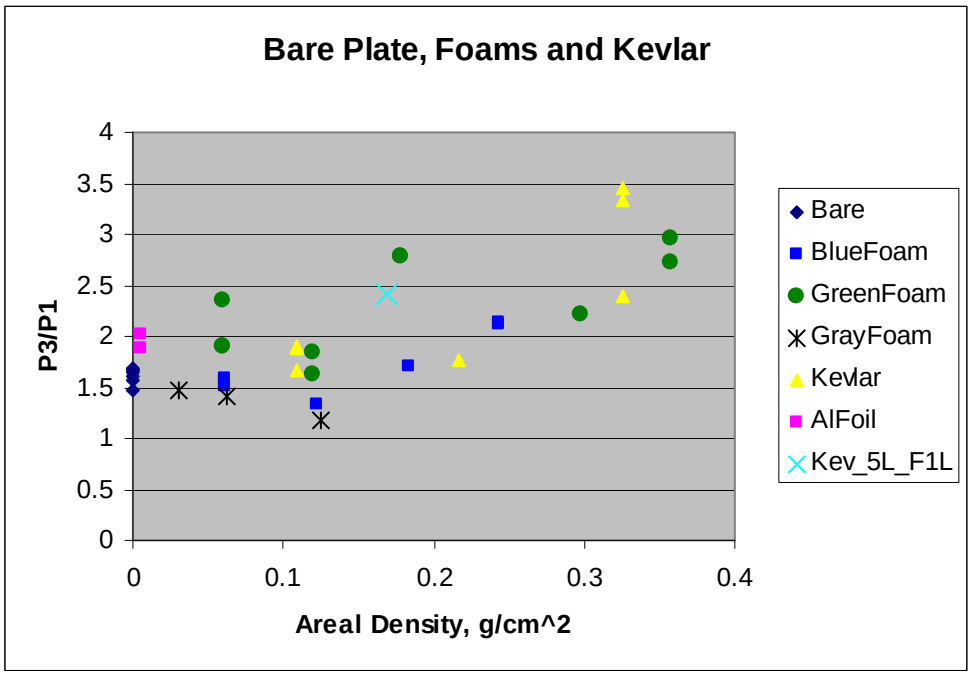

Figure 6: Plot of the ratio of the reflected pressure measured by the flush mounted sensor in the endplate to the incident side-on pressure measured at Sensor 1.

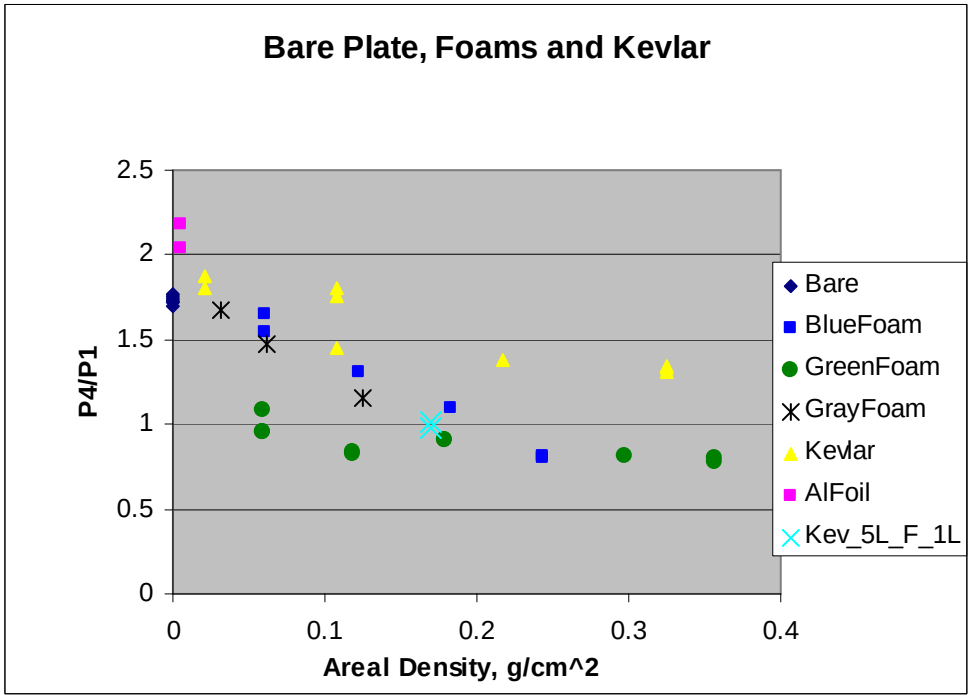

Figure 7: Plot of the ratio of the reflected pressure measured by the recessed sensor in the endplate to the incident side-on pressure measured at Sensor 1.

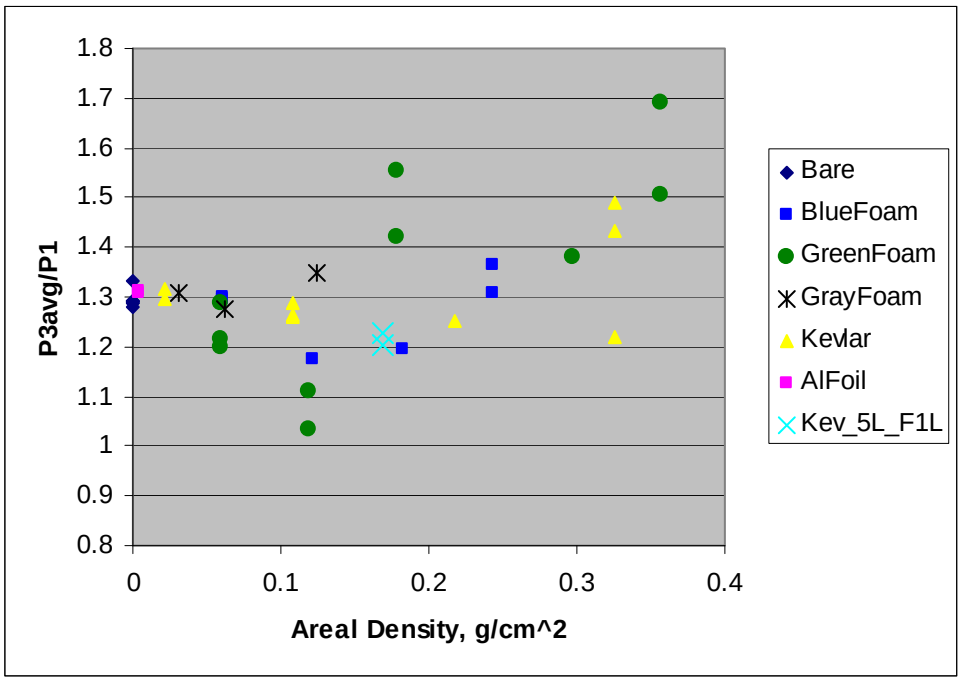

Figure 8: Plot of the normalized average pressure, taken between the initial peak pressure and the arrival time of the expansion wave, for the flush mounted sensor.

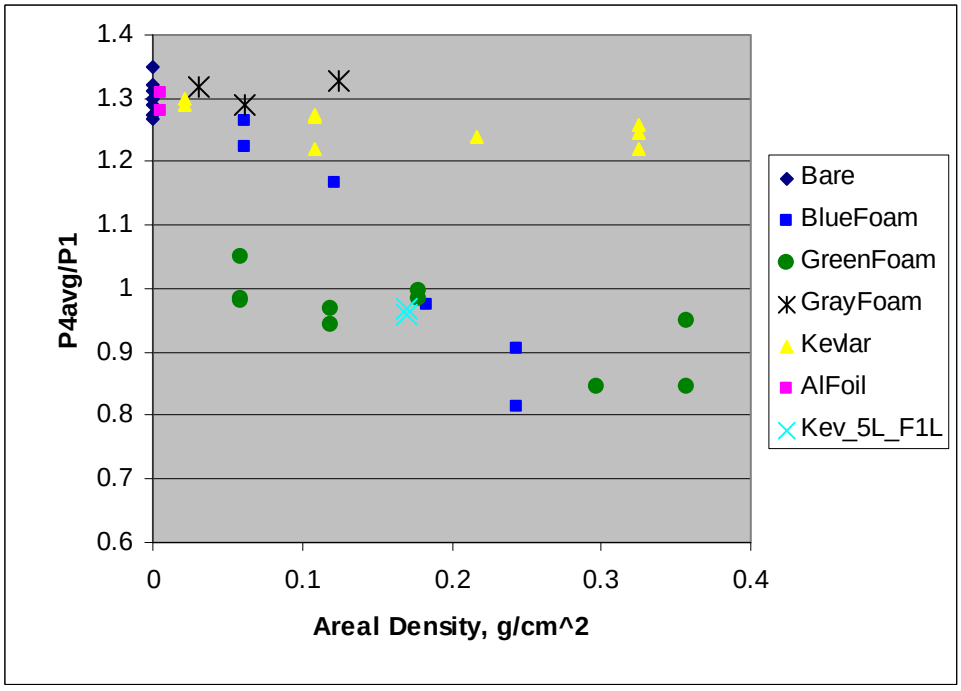

Figure 9: Plot of the normalized average pressure, taken between the peak pressure and the arrival time of the expansion wave, for the recessed sensor.

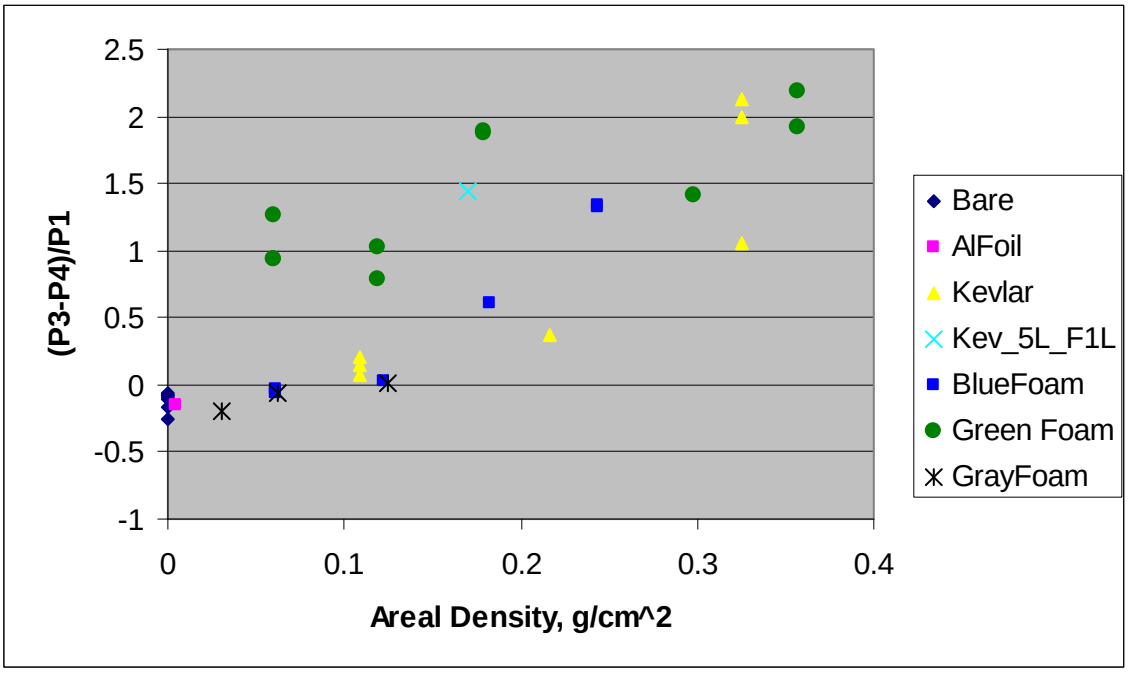

Figure 10: Plot of the difference in peak pressure between the flush mounted sensor (P3) and the recessed sensor (P4) normalized by the pressure at Sensor 1.

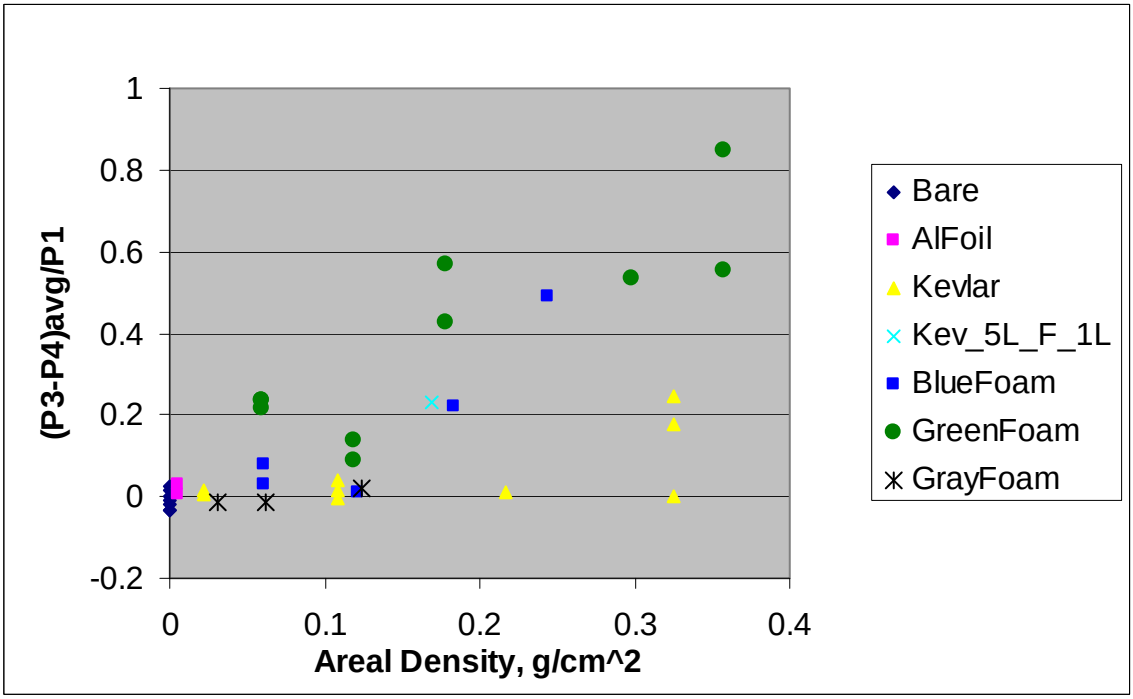

Figure 11: Plot of the difference in average pressure between the flush mounted sensor (P3) and the recessed sensor (P4) normalized by the pressure at Sensor 1.

The bar graph in Figure 12: shows the behavior of the different materials and of a given material at different areal densities. The last column (K5LF-1L2) is for five layers of Kevlar® backed by 0.25 in. of blue foam. In this graph, all tests at a given condition were averaged if both the peak

pressures P3 and P4 were properly recorded (not clipped). Some cases had as many as six trials while others had only one. The materials and the number of replications used for each test condition are listed in Table 3. It is clear from Figure 12: that both the material and its thickness for the peak and average pressure were measured differently by the two sensors.

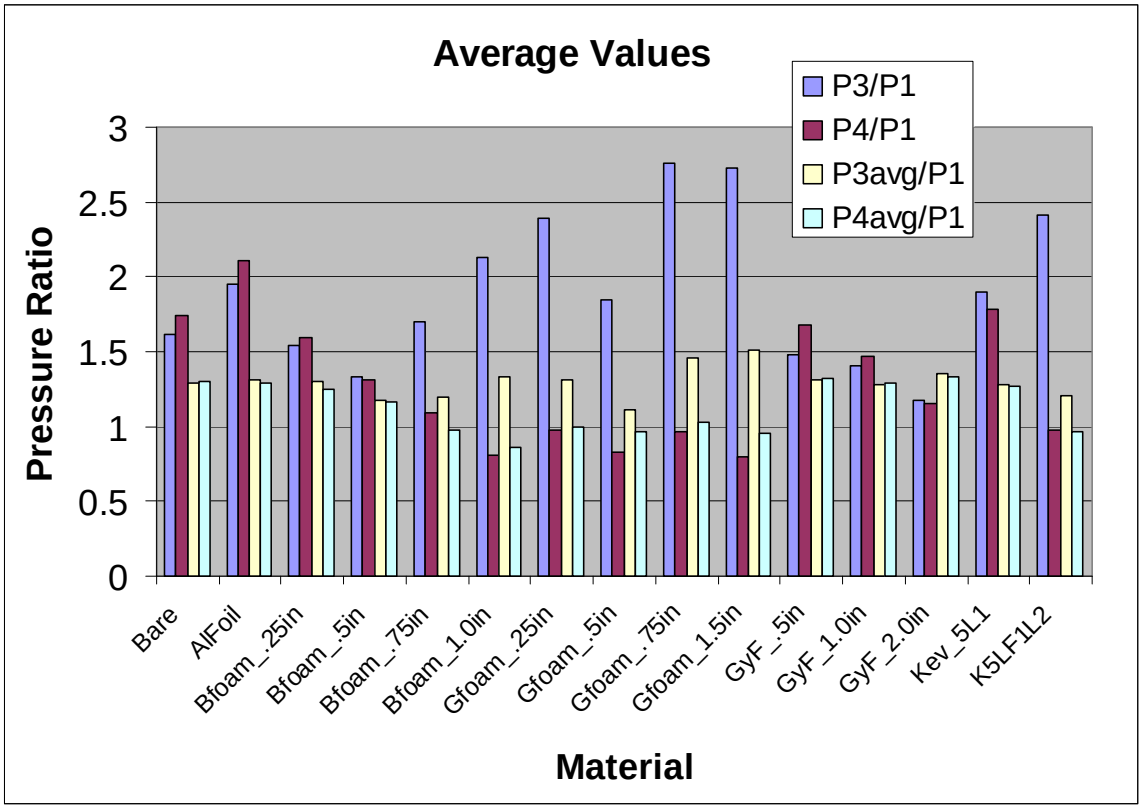

Figure 12: Average values for both the peak and average pressure ratios for all conditions evaluated.

The data from the recessed sensor seem logical at first glance since the monotonic decrease with increasing areal density (thickness) is reasonable. However, any cavity such as the 2 mm recess limits the frequency content of any signal that passes through the cavity. A general rule sets the limiting frequency at one-tenth of the resonant frequency of the cavity. This resonant frequency is given by c/4L, where L is the length of the cavity and c is the speed of sound. For L = 2 mm the resonant frequency is 43 kHz, which means that frequencies above 43 kHz would not be included. The rapid rise in pressure at all sensors when the endplate was uncovered suggests that many frequencies above this level were part of the shock wave. Thus, a recessed sensor may not read the correct pressure values.

The pressure response from the flush mounted sensor seems at first to be problematic. It started with an initial decrease, or remained constant, as the areal density was increased, and then increased significantly as the areal density was increased further. However, Nesterenko [11] has shown both theoretically and with experiments that porous materials can be compressed by a shock wave. The compressed material may then release the stored energy at the same time the shock wave reaches the endplate. This energy release augments the pressure with the overall

result being that the porous material enhances the downstream pressure rather than providing the expected pressure attenuation. Nesterenko gives a critical value, based on the mechanical properties of the material, above which attenuation would be expected. It is possible, even though the shock wave was rather weak, that some compression of the material occurred. If this happened Nesterenko's arguments could apply to the materials reported here (Figures 6 and 8). If so, this critical value was not reached in any of the tests conducted as measured by the flush mounted sensors.

5 Conclusions

Several analyses were performed to correlate theoretical calculations with the observed measurements. Theoretical calculations of shock strength determined from the driving pressure agree well with the shock strength calculated from the side-on pressure downstream from the diaphragm. Shock speed determined from transit times is in excellent agreement with the shock speed determined from the shock pressure ratio. Reflected pressures, both at the endplate and at the side-on pressure taps, agree with expected values. This indicates that the shock tube was working properly and that all sensors were responding appropriately.

The plots in Figures 6 through 11 show that a sensor recessed relative to a reflecting surface gives different values for the reflected pressure than a sensor mounted flush with the reflecting surface. Arguments have been given that provide at least a partial explanation of these findings, but more work is needed to obtain the definitive answer to this problem. Well characterized foams and a wider selection of flexible fabrics in a greater range of thicknesses would determine the validity of Nesterenko's theory for materials of interest.

The present information suggests that careful consideration must be given to appropriate mounting of materials with respect to pressure sensors for measurement. Degree of contact between sensor and material may have a significant effect on results.

This document reports research undertaken at the U.S. Army Natick Soldier Research, Development and Engineering Center, Natick, MA, and has been assigned No. NATICK/TR- 09 / 010 in a series of reports approved for publication.

6 References

1. Phan, K.C.a.J.L.S., *On the effects of shock wave reflection in a confined space.*, in *International Symposium on Shock Tubes and Waves. Shock tubes and waves.* 1985, Magnes Press: Jerusalem. p. 139-145.
2. Skews, B.W., *Pressure Amplificationn Due to Clothing (final)*. 2001, School of Mechanical, Aeronautical, and Industrial Engineering, Univ. of the Witwaterstrand: Johannesburg. p. 56.
3. Skews, B.W.a.S.B., *Blast pressure Amplification due to Textile Coverings.* Textile Research Journal, 2006. **76**(4): p. 328-335.
4. Gelfand, B.E., A.V. Gubanov, and E.I. Timofeev, *Interaction of Shock Waves in Air with a Porous Screen*. 1984: Moscow. p. 6.
5. Gibson, P.W., *Amplification of Air Shock Waves by Textile Materials.* Journal of the Textile Institute, 1995. **86**(1): p. 119-128.
6. Winfree, N.A.a.J.H.K., *Blast Mitigation Jacket for Training*. 2006, Dominca, Inc.: Albuquerque, New Mexico. p. 80pp.
7. Wright, J.R., *Shock Tubes; Chapter 3, Theory of the Shock Tube*. 1961, London & Colchester, Great Britain: Spottiswoode, Ballantyne & Co. Ltd.
8. LaPlante, D., P.R. Smith and W.S. Gregory, *Ventilation System Pressure Transients, Small-Scale Shock Tube Results*. 1979, New Mexico State University, Dept. of Mechanical Engineering: University Park, NM. p. 16 pages.
9. Thompson, P.A., *Compressible Fluid Dynamics*. 1972 ed. Advanced Engineering Series, ed. I.H. Shames. 1972, San Fransisco: McGraw-Hill Book Company. 560.
10. Beranek, L.L., *Noise Reduction*. Prepared for a Special Summer Program at MIT. 1960, Boston, MA: McGraw-Hill Book Company, Inc. New York, Toronto, London.
11. Nesterenko, V.F., *Shock (Blast) Mitigation by "Soft" Condensed Matter.* Mat. Res. Soc. Symp. Proc., 2003. **759**: p. 12 pages.